



HAL
open science

GPS Multipath Induced Errors for the Vector Tracking Loop: Insight into Multipath Detection

Elie Amani, Jean-Rémi de Boer, Willy Vigneau, Karim Djouani, Anish Kurien

► **To cite this version:**

Elie Amani, Jean-Rémi de Boer, Willy Vigneau, Karim Djouani, Anish Kurien. GPS Multipath Induced Errors for the Vector Tracking Loop: Insight into Multipath Detection. 2016 European Navigation Conference (ENC 2016), May 2016, Helsinki, Finland. hal-01570371

HAL Id: hal-01570371

<https://hal.science/hal-01570371>

Submitted on 29 Jul 2017

HAL is a multi-disciplinary open access archive for the deposit and dissemination of scientific research documents, whether they are published or not. The documents may come from teaching and research institutions in France or abroad, or from public or private research centers.

L'archive ouverte pluridisciplinaire **HAL**, est destinée au dépôt et à la diffusion de documents scientifiques de niveau recherche, publiés ou non, émanant des établissements d'enseignement et de recherche français ou étrangers, des laboratoires publics ou privés.

GPS Multipath Induced Errors for the Vector Tracking Loop: Insight into Multipath Detection

Elie Amani ⁽¹⁾⁽²⁾⁽³⁾, Jean-Rémi De Boer ⁽²⁾, Willy Vigneau ⁽²⁾

⁽¹⁾LISSI Laboratory, Université Paris-Est Créteil (UPEC)
Paris, France
⁽²⁾M3 Systems
Toulouse, France

Karim Djouani ⁽¹⁾⁽³⁾, Anish Kurien ⁽³⁾

⁽¹⁾LISSI Laboratory, Université Paris-Est Créteil (UPEC)
Paris, France
⁽³⁾F*SATI/Dept. of Electrical Engineering, Tshwane University
of Technology (TUT)
Pretoria, South Africa

Abstract— Multipath is one of the most serious sources of error in the Global Positioning System (GPS). Multipath distorts the correlation function used for carrier phase and code delay measurements, and therefore induces errors in these measurements and consequently in the calculated positioning solution. This paper aims at characterizing multipath induced tracking errors for a vector tracking loop (VTL). The paper contributes to the characterization of tracking and positioning errors for VTLs by deriving models that allow the analysis of both code and carrier tracking errors with respect to multipath delay, multipath phase and multipath fading frequency. The paper further provides a simple multipath detection technique based on correlator outputs, showing another advantage of the VTL over the scalar tracking loop (STL).

Index Terms—GPS, multipath, tracking error, vector tracking loop, multipath detection.

I. INTRODUCTION

The Global Positioning System (GPS) has been designed in such a way as to use a clear line-of-sight (LOS) between the receiver and the satellites it is tracking to compute the positioning solution. But with the ubiquity of GPS receivers, they are found in more and more constrained environments with LOS reflecting and/or blocking obstacles. Such environments include heavy foliage, urban canyon, and indoor areas. Multipath (MP) is any signal that has been reflected or diffracted at least once before being incident to the GPS receiver's antenna. The blending of the LOS signal with one or more MP signals induces tracking errors in the receiver's channels. Be it specular, diffuse or diffracted [1], multipath has the same effect, which is the distortion of the correlation function used for carrier phase and code delay measurements, and therefore the distortion of these measurements. To better grasp this, it is important to understand what signal tracking in a GPS receiver entails. Tracking consists of aligning a local replica of the carrier and the spreading code with the incoming signal's carrier and code for the satellite of interest. These

alignments are achieved based on correlation between the local replica and incoming signal using scalar tracking loops (STLs) such as code delay, carrier phase and/or frequency locked loops, or vector tracking loops (VTLs) such as the vector delay frequency locked loop (VDFLL). The tracking and navigation functions are combined in a VTL via an algorithm such as the Extended Kalman Filter (EKF), the Unscented Kalman Filter (UKF) or the Particle Filter (PF). The navigation solution (position-velocity-time or PVT) is derived from all tracking channels results. The VTL structure can track temporarily attenuated or blocked satellite signals because the navigation solution can be obtained from other visible satellites. However, it has the weakness of propagating errors from a disturbed channel to all other tracking channels as they are dependent on one another. In the presence of multipath, the loops (STL or VTL) are not tracking the LOS signal anymore but rather the LOS blended with delayed copies. Thus, multipath contributes significantly to the error induced in the tracking and consequently in the positioning solution.

To better design multipath detection and mitigation techniques, it is important to study the characteristics of multipath on a theoretical point of view. This paper aims at providing characterization of multipath induced tracking errors in the context of VTLs. The paper covers code delay, carrier phase and carrier frequency tracking errors. The topic has been extensively covered for STLs in existing literature [2] [3] [4] [5] but not much for VTLs. In fact, VTLs have been largely addressed in literature to explain their performance benefits over STLs in degraded signal environments affected by multipath, scintillations and interference [6] [7] [8] [9] [10] but without a theoretical analysis of multipath induced errors. In [2] and many other publications in literature, only the envelope models are used for code delay errors. The mathematical expressions of the errors under the envelope are presented in [3] [4] and [5]. In [3], the carrier phase tracking error is analysed under the assumption that the code delay tracking error is zero, which is not accurate since the code delay tracking error is nonzero in the presence of multipath. The models in [4] and [5] overcome this weakness. Recently, a

paper that characterizes the effects of multipath on the VTL and provides theoretical error expressions was published [11]. It is proved in [11] that multipath induced tracking error is reduced by the VTL algorithm when more than four satellites are tracked. This paper contributes by extension from models in [11] to the characterization of code delay and carrier phase and frequency tracking errors for VTLs by deriving models that allow the analysis of both code and carrier tracking errors with respect to multipath delay, multipath phase and multipath fading frequency. The paper further provides a simple multipath detection technique for the VTL based on correlator outputs.

The rest of the paper is organized as follows. In section II, the models of correlator outputs in the presence of multipath are described. Section III derives code and carrier tracking error models. Section IV provides an analysis for devising multipath detection techniques based on correlator outputs and provides one such detection technique validated with simulations. Finally section V gives concluding remarks.

II. CORRELATOR OUTPUTS IN THE PRESENCE OF MULTIPATH

If a specular multipath model with a finite number of multipath signals is considered, the signal entering the code and phase loop, neglecting the low rate data, can be expressed as:

$$x(t) = A_0 C(t - \tau_0) \cos(\omega t - \varphi_0) + \sum_{l=1}^L A_l C(t - \tau_l) \cos(\omega t - \varphi_l) + w(t) \quad (1)$$

where L is the number of multipath signals, A_0 and A_l are the LOS and l^{th} multipath amplitudes respectively, $C(t)$ is the spreading code, τ_0 , τ_l , φ_0 , φ_l are the time and phase delays induced by the transmission from satellite to receiver for the LOS and l^{th} multipath signals respectively, ω is the nominal GPS L1, L2 or L5 radial frequency, and $w(t)$ is the zero-mean additive white Gaussian noise with variance σ^2 . If a one-multipath model is used, the signal entering the code and phase loops can be expressed as:

$$x(t) = A_0 C(t - \tau_0) \cos(\omega t - \varphi_0) + A_M C(t - \tau_M) \cos(\omega t - \varphi_M) + w(t) \quad (2)$$

If A_M is written as $A_M = \alpha A_0$, the in-phase and quadrature outputs of the prompt correlator in the presence of a specular multipath, at an instant of time, are:

$$\begin{aligned} I_p &= A_0 R(\Delta\tau) \cos(\Delta\varphi) + \\ &\alpha A_0 R(\Delta\tau - \delta_M) \cos(\Delta\varphi - \theta_M) + w_{I,p} \\ Q_p &= A_0 R(\Delta\tau) \sin(\Delta\varphi) + \\ &\alpha A_0 R(\Delta\tau - \delta_M) \sin(\Delta\varphi - \theta_M) + w_{Q,p} \end{aligned} \quad (3)$$

where R is the autocorrelation function, $\Delta\tau$ is the error between the LOS signal delay and the estimated code replica delay, $\Delta\varphi$ is the error between the LOS carrier phase and the estimated carrier replica phase, $\delta_M = \tau_M - \tau_0$ is the delay of the multipath M with respect to the LOS, $\theta_M = \varphi_M - \varphi_0$ is the

phase shift of multipath M with respect to the LOS, and $w_{X,p}$ is the post-correlation noise. δ_M is always positive since the multipath signal always arrives later than the LOS signal. Similarly, the early and late in-phase and quadrature correlator outputs are:

$$\begin{aligned} I_E &= A_0 R(\Delta\tau + d) \cos(\Delta\varphi) + \\ &\alpha A_0 R(\Delta\tau - \delta_M + d) \cos(\Delta\varphi - \theta_M) + w_{I,E} \\ Q_E &= A_0 R(\Delta\tau + d) \sin(\Delta\varphi) + \\ &\alpha A_0 R(\Delta\tau - \delta_M + d) \sin(\Delta\varphi - \theta_M) + w_{Q,E} \end{aligned} \quad (4)$$

$$\begin{aligned} I_L &= A_0 R(\Delta\tau - d) \cos(\Delta\varphi) + \\ &\alpha A_0 R(\Delta\tau - \delta_M - d) \cos(\Delta\varphi - \theta_M) + w_{I,L} \\ Q_L &= A_0 R(\Delta\tau - d) \sin(\Delta\varphi) + \\ &\alpha A_0 R(\Delta\tau - \delta_M - d) \sin(\Delta\varphi - \theta_M) + w_{Q,L} \end{aligned} \quad (5)$$

where d is half the Early-Late correlator chip spacing ∂ ($d = \partial/2$, $0 < \partial \leq 1$).

III. CARRIER AND CODE TRACKING ERROR MODELS

The code and carrier tracking errors of the VDFLL can be analysed at two stages, an initial stage and a steady-state stage. The EKF-based VDFLL uses code and frequency discrimination outputs as measurements directly. Once the scalar DFLL (SDFLL) is locked and the initial PVT solution is calculated, the receiver can switch to VDFLL and use the steady-state SDFLL measurement errors as its initial VDFLL measurement errors. When the tracking loop enters VDFLL mode, both code and carrier tracking errors get smaller and smaller and gradually approach their steady-state values. The tracking errors obtained from the SDFLL measurements therefore constitute the maximum VDFLL tracking errors.

A. Initial VDFLL Carrier Frequency Tracking Error

The frequency tracking error that is derived and analysed in this section corresponds to the steady-state frequency tracking error of a scalar frequency locked loop (FLL). The arctangent frequency discriminator generates an estimated Doppler deviation between the received signal and the replica signal using the following expression [12] [9]:

$$Discr(\Delta f) = \frac{\arctan(CROSS / DOT)}{2\pi(t_2 - t_1)} \quad (6)$$

$$\begin{aligned} \text{where } DOT &= I_{p1} \times I_{p2} + Q_{p1} \times Q_{p2} \\ CROSS &= I_{p1} \times Q_{p2} - I_{p2} \times Q_{p1} \end{aligned}$$

In the absence of multipath, the following Prompt correlator outputs can be defined between two Integrate and Dump instants t_1 and t_2 ignoring post-correlation noise:

$$\begin{aligned} I_{p1} &= A_0 R(\Delta\tau) \cos(\Delta\varphi_1) ; I_{p2} = A_0 R(\Delta\tau) \cos(\Delta\varphi_2) ; \\ Q_{p1} &= A_0 R(\Delta\tau) \sin(\Delta\varphi_1) ; Q_{p2} = A_0 R(\Delta\tau) \sin(\Delta\varphi_2) \end{aligned} \quad (7)$$

The FLL is in lock when the Doppler deviation $Discr(\Delta f) = 0$. Substituting Eq. (7) into DOT and $CROSS$ expressions, the ratio $CROSS / DOT = \frac{\sin(\Delta\varphi_2 - \Delta\varphi_1)}{\cos(\Delta\varphi_2 - \Delta\varphi_1)} = \tan(\Delta\varphi_2 - \Delta\varphi_1)$.

Let $\Delta\varphi_2 - \Delta\varphi_1 = 2\pi\Delta f_D T$, where $T = t_2 - t_1$ and Δf_D is the Doppler frequency residual of the LOS signal or the Doppler frequency error between LOS and replica signals.

$$Discr(\Delta f) = 0 \text{ when } \frac{\arctan[\tan(2\pi\Delta f_D T)]}{2\pi(t_2 - t_1)} = 0, \text{ i.e. } \Delta f_D = 0.$$

In the presence of multipath, the locking conditions remain the same but they induce a different frequency residual. The slope of the curve representing the frequency discriminator operation in its linear range is not 1 anymore. This induces error in the carrier frequency tracking. If the multipath fading effect is considered, the following Prompt correlator outputs can be defined between two Integrate and Dump instants t_1 and t_2 ignoring post-correlation noise:

$$\begin{aligned} I_{P1} &= A_0 R(\Delta\tau) \cos(\Delta\varphi_1) + \alpha A_0 R(\Delta\tau - \delta_M) \cos(\Delta\tilde{\varphi}_1 - \theta_M) \\ I_{P2} &= A_0 R(\Delta\tau) \cos(\Delta\varphi_2) + \alpha A_0 R(\Delta\tau - \delta_M) \cos(\Delta\tilde{\varphi}_2 - \theta_M) \\ Q_{P1} &= A_0 R(\Delta\tau) \sin(\Delta\varphi_1) + \alpha A_0 R(\Delta\tau - \delta_M) \sin(\Delta\tilde{\varphi}_1 - \theta_M) \\ Q_{P2} &= A_0 R(\Delta\tau) \sin(\Delta\varphi_2) + \alpha A_0 R(\Delta\tau - \delta_M) \sin(\Delta\tilde{\varphi}_2 - \theta_M) \end{aligned} \quad (8)$$

where $\alpha = A_M / A_0$, $\Delta\tilde{\varphi}_1$ and $\Delta\tilde{\varphi}_2$ are affected by a fading frequency component $f_F = \frac{d(\varphi_M)}{dt} / 2\pi$ due to multipath. Substitution of Eq. (8) into DOT and $CROSS$ expressions yields after trigonometric manipulations:

$$\begin{aligned} DOT &= A_0^2 R^2(\Delta\tau) \cos(\Delta\varphi_2 - \Delta\varphi_1) + \alpha^2 A_0^2 R^2(\Delta\tau - \delta_M) \cos(\Delta\tilde{\varphi}_2 - \Delta\tilde{\varphi}_1) \\ &+ \alpha A_0^2 R(\Delta\tau) R(\Delta\tau - \delta_M) [\cos(\Delta\tilde{\varphi}_2 - \Delta\varphi_1) \cos\theta_M + \sin(\Delta\tilde{\varphi}_2 - \Delta\varphi_1) \sin\theta_M] \\ &+ \alpha A_0^2 R(\Delta\tau) R(\Delta\tau - \delta_M) [\cos(\Delta\varphi_2 - \Delta\tilde{\varphi}_1) \cos\theta_M - \sin(\Delta\varphi_2 - \Delta\tilde{\varphi}_1) \sin\theta_M] \\ CROSS &= A_0^2 R^2(\Delta\tau) \sin(\Delta\varphi_2 - \Delta\varphi_1) + \alpha^2 A_0^2 R^2(\Delta\tau - \delta_M) \sin(\Delta\tilde{\varphi}_2 - \Delta\tilde{\varphi}_1) \\ &+ \alpha A_0^2 R(\Delta\tau) R(\Delta\tau - \delta_M) [\sin(\Delta\tilde{\varphi}_2 - \Delta\varphi_1) \cos\theta_M - \cos(\Delta\tilde{\varphi}_2 - \Delta\varphi_1) \sin\theta_M] \\ &+ \alpha A_0^2 R(\Delta\tau) R(\Delta\tau - \delta_M) [\sin(\Delta\varphi_2 - \Delta\tilde{\varphi}_1) \cos\theta_M + \cos(\Delta\varphi_2 - \Delta\tilde{\varphi}_1) \sin\theta_M] \end{aligned} \quad (9)$$

Let $\Delta\tilde{\varphi}_2 - \Delta\tilde{\varphi}_1 = 2\pi\Delta\tilde{f}_D T$; $\Delta\tilde{f}_D = \Delta f_D + f_F$;

$$\Delta\tilde{\varphi}_2 - \Delta\varphi_1 = \Delta\varphi_2 - \Delta\tilde{\varphi}_1 = 2\pi \frac{\Delta f_D + \Delta\tilde{f}_D}{2} T = \pi(\Delta f_D + \Delta\tilde{f}_D) T; \quad (10)$$

$$\alpha = \frac{A_M}{A_0} = \frac{\sqrt{2T(C/N_0)_M \sin^2[\pi(\Delta f_D + f_F)T]}}{\sqrt{2T(C/N_0) \sin^2(\pi\Delta f_D T)}} = \sqrt{\gamma} \frac{\sin c(\pi\Delta\tilde{f}_D T)}{\sin c(\pi\Delta f_D T)}$$

where $\gamma = M / D$ ($0 < \gamma < 1$) is the multipath to LOS (direct signal) power ratio, $\Delta\tilde{f}_D$ is the Doppler frequency residual of the multipath signal or the Doppler frequency error between multipath and replica signals, and f_F is the fading frequency due to multipath. Equations (9) therefore become:

$$DOT = A_0^2 R^2(\Delta\tau) \cos(2\pi\Delta f_D T) + \alpha^2 A_0^2 R^2(\Delta\tau - \delta_M) \cos(2\pi\Delta\tilde{f}_D T) + 2\alpha A_0^2 R(\Delta\tau) R(\Delta\tau - \delta_M) \cos[\pi(\Delta f_D + \Delta\tilde{f}_D)T] \cos\theta_M \quad (11)$$

$$CROSS = A_0^2 R^2(\Delta\tau) \sin(2\pi\Delta f_D T) + \alpha^2 A_0^2 R^2(\Delta\tau - \delta_M) \sin(2\pi\Delta\tilde{f}_D T) + 2\alpha A_0^2 R(\Delta\tau) R(\Delta\tau - \delta_M) \sin[\pi(\Delta f_D + \Delta\tilde{f}_D)T] \cos\theta_M \quad (12)$$

In the presence of multipath, the FLL is in lock still when the discriminator output is zero, i.e. when $Discr(\Delta f) = 0$. Let $X = CROSS / DOT$.

$$\begin{aligned} X &= \frac{\sin(2\pi\Delta f_D T) + \alpha^2 \beta^2 \sin(2\pi\Delta\tilde{f}_D T) + 2\alpha\beta \sin[\pi(\Delta f_D + \Delta\tilde{f}_D)T] \cos\theta_M}{\cos(2\pi\Delta f_D T) + \alpha^2 \beta^2 \cos(2\pi\Delta\tilde{f}_D T) + 2\alpha\beta \cos[\pi(\Delta f_D + \Delta\tilde{f}_D)T] \cos\theta_M} \\ X &= \frac{\sin(2\pi\Delta f_D T) + \alpha^2 \beta^2 \sin[2\pi(\Delta f_D + f_F)T] + 2\alpha\beta \sin[\pi(2\Delta f_D + f_F)T] \cos\theta_M}{\cos(2\pi\Delta f_D T) + \alpha^2 \beta^2 \cos[2\pi(\Delta f_D + f_F)T] + 2\alpha\beta \cos[\pi(2\Delta f_D + f_F)T] \cos\theta_M} \\ X &= \frac{\left[\tan(2\pi\Delta f_D T) + \alpha^2 \beta^2 \tan(2\pi\Delta\tilde{f}_D T) \cos(2\pi f_F T) + \alpha^2 \beta^2 \sin(2\pi f_F T) \right]}{\left[1 + \alpha^2 \beta^2 \cos(2\pi f_F T) - \alpha^2 \beta^2 \tan(2\pi\Delta f_D T) \sin(2\pi f_F T) \right]} \\ &\quad \left[1 + \alpha^2 \beta^2 \cos(2\pi f_F T) + 2\alpha\beta \cos(\pi f_F T) \cos\theta_M \right]}{\left[1 + \alpha^2 \beta^2 \cos(2\pi f_F T) + 2\alpha\beta \cos(\pi f_F T) \cos\theta_M \right]} \\ X &= \frac{\tan(2\pi\Delta f_D T) + \frac{\alpha^2 \beta^2 \sin(2\pi f_F T) + 2\alpha\beta \sin(\pi f_F T) \cos\theta_M}{1 + \alpha^2 \beta^2 \cos(2\pi f_F T) + 2\alpha\beta \cos(\pi f_F T) \cos\theta_M}}{1 - \tan(2\pi\Delta f_D T) \frac{\alpha^2 \beta^2 \sin(2\pi f_F T) + 2\alpha\beta \sin(\pi f_F T) \cos\theta_M}{1 + \alpha^2 \beta^2 \cos(2\pi f_F T) + 2\alpha\beta \cos(\pi f_F T) \cos\theta_M}} \end{aligned} \quad (13)$$

Let $\tan \Omega = \frac{\alpha^2 \beta^2 \sin(2\pi f_F T) + 2\alpha\beta \sin(\pi f_F T) \cos\theta_M}{1 + \alpha^2 \beta^2 \cos(2\pi f_F T) + 2\alpha\beta \cos(\pi f_F T) \cos\theta_M}$, and Eq. (13) becomes [11]:

$$X = \frac{\tan(2\pi\Delta f_D T) + \tan \Omega}{1 - \tan(2\pi\Delta f_D T) \tan \Omega} = \tan(2\pi\Delta f_D T + \Omega) \quad (14)$$

The VFLL is in lock when $X = 0$, meaning when $\tan(2\pi\Delta f_D T + \Omega) = 0$, i.e. when:

$$2\pi\Delta f_D T + \Omega = 0 \quad (15)$$

The associated Doppler frequency error is no longer zero:

$$\Delta f_D = -\frac{\Omega}{2\pi T} \quad (16)$$

The pseudorange rate (velocity) measurement error associated with a multipath induced frequency tracking error Δf_D is [11] [9]:

$$\Delta \dot{\rho} = -\frac{c}{f_L} \Delta f_D \quad (17)$$

where f_L is the nominal GPS L1, L2 or L5 carrier frequency.

B. Initial VDFLL Code Delay Tracking Error

The VDFLL is often implemented with a normalised non-coherent Early-minus-Late (EmL) Envelope code discriminator as in Eq. (18) or a normalized non-coherent EmL Power (EmLP) code discriminator as in Eq. (19).

$$\text{Discr}(\Delta\tau) = \frac{\sum \sqrt{I_E^2 + Q_E^2} - \sum \sqrt{I_L^2 + Q_L^2}}{\sum \sqrt{I_E^2 + Q_E^2} + \sum \sqrt{I_L^2 + Q_L^2}} \quad (18)$$

$$\text{Discr}(\Delta\tau) = \frac{(I_E^2 + Q_E^2) - (I_L^2 + Q_L^2)}{(I_E^2 + Q_E^2) + (I_L^2 + Q_L^2)} \quad (19)$$

The non-coherent EmLP delay locked loop (DLL) discriminator output in the presence of multipath is:

$$\begin{aligned} \text{EmLP} &= I_E^2 + Q_E^2 - I_L^2 - Q_L^2, \\ \text{EmLP} &= A_0^2 \left[R^2(\Delta\tau + d) - R^2(\Delta\tau - d) \right] + \\ &\quad \alpha^2 A_0^2 \left[R^2(\Delta\tau - \delta_M + d) - R^2(\Delta\tau - \delta_M - d) \right] + \\ &\quad 2\alpha A_0^2 \left[\frac{R(\Delta\tau + d)R(\Delta\tau - \delta_M + d)}{R(\Delta\tau - d)R(\Delta\tau - \delta_M - d)} \right] \cos\theta_M. \end{aligned} \quad (20)$$

The EmLP discriminator produces the following MP induced error, which is the initial VDFLL delay error [3] [4]:

$$\begin{aligned} \Delta\tau &= \begin{cases} \frac{\alpha[\alpha + \cos\theta_M]\delta_M}{1 + 2\alpha\cos\theta_M + \alpha^2}, \text{ for} \\ 0 \leq \delta_M < \frac{1 + 2\alpha\cos\theta_M + \alpha^2}{2[1 + \alpha\cos\theta_M]} \end{cases} \\ &\quad \left\{ \begin{aligned} &\left[\frac{[\alpha\cos\theta_M(1 - \delta_M) - \alpha^2 d + 1 - d]^2 +}{2\alpha^2 \delta \cos\theta_M [\cos\theta_M(1 - d) + \alpha(1 - \delta_M)]} \right]^{1/2} \\ & - [\alpha\cos\theta_M(1 - \delta_M) - \alpha^2 d + 1 - d] \end{aligned} \right\}, \text{ for} \\ &\quad \frac{1 + 2\alpha\cos\theta_M + \alpha^2}{2[1 + \alpha\cos\theta_M]} \leq \delta_M < \frac{(1 + \alpha\delta\cos\theta_M)(2 - \delta) - \delta(1 - d - \alpha^2 d)}{\alpha\delta\cos\theta_M + 2 - \delta} \\ &\quad \left\{ \begin{aligned} &\left[\frac{\alpha^2 \delta_M^2 \cos^2\theta_M + 2\alpha(2 - \delta)(\alpha - \cos\theta_M)\delta_M}{4\alpha^2(\delta^2/4 - \sin^2\theta_M) - 4\alpha^2\delta_M \cos^2\theta_M +} \right]^{1/2} \\ & (2 - \delta)(2 - \delta + 2\alpha\delta\cos\theta_M) \end{aligned} \right\} \\ &\quad \left. \frac{(\alpha\cos\theta_M - \alpha^2)\delta_M + \alpha^2(1 + d) - \alpha\delta\cos\theta_M - 2 + \delta}{2\alpha\cos\theta_M - \alpha^2} \right\}, \text{ for} \\ &\quad \frac{(1 + \alpha\delta\cos\theta_M)(2 - \delta) - \delta(1 - d - \alpha^2 d)}{\alpha\delta\cos\theta_M + 2 - \delta} \leq \delta_M < 1 + d. \\ &\quad 0, \text{ for } \delta_M \geq 1 + d. \end{cases} \quad (21)$$

The pseudorange measurement error corresponding to a multipath induced code delay tracking error $\Delta\tau$ is [11] [13]:

$$\Delta\rho = -\frac{c}{R_C} \Delta\tau \quad (22)$$

where R_C is the code chip rate and c is the speed of light.

Figures 1 and 3 show the frequency and delay tracking errors of the VDFLL and the phase tracking error [4] of the phase locked loop (PLL) that assists it. The non-coherent EmLP code discriminator and the standard correlator chip spacing ($d = 0.5$) are used. The errors are displayed versus multipath

delay and multipath fading frequency in Fig. 1 and versus multipath phase and multipath fading frequency in Fig. 2, with $\theta_M = 2\pi f_{L1}\delta_M / R_C$. The VDFLL is in its initial tracking state so these errors are the maximum there can be for the given multipath delay and phase values. The values of delay tracking errors displayed in terms of multipath phase in Fig. 3(c) and Fig. 2 are small because they are computed for multipath delay values very close to zero with the relationship $\theta_M = 2\pi f_{L1}\delta_M / R_C$ taken into account. They evolve in amplitude like in Fig. 1(c) for increasing multipath delay values. However, as depicted, Fig. 3(c) and Fig. 2 show that maximal delay errors occur for multipath phase values $\theta_M = 0^\circ + k360^\circ$ and $\theta_M = 180^\circ + k360^\circ$, with k being an integer.

C. Steady-state VDFLL Code and Carrier Tracking Errors

The steady-state code and carrier tracking errors of a VDFLL based on EKF are analysed. Let this VDFLL EKF's state vector be denoted as

$$X = [\delta x, \delta y, \delta z, \delta \dot{x}, \delta \dot{y}, \delta \dot{z}, \delta t, \delta \dot{t}]^T \quad (23)$$

where the vector's elements are the errors in estimating the receiver's position, velocity, clock bias and clock drift.

Let the measurement vector be

$$Y = [\delta\rho_1, \delta\rho_2, \dots, \delta\rho_N, \delta\dot{\rho}_1, \delta\dot{\rho}_2, \dots, \delta\dot{\rho}_N]^T \quad (24)$$

Its elements are the code and frequency discriminators results for the N tracking channels. The system model is:

$$\begin{aligned} X_k &= \Phi X_{k-1} + W_{k-1} \\ Y_k &= H_k X_k + V_k \end{aligned} \quad \text{where}$$

$$\Phi = \begin{bmatrix} I_{3 \times 3} & T I_{3 \times 3} & 0_{3 \times 2} \\ 0_{3 \times 3} & I_{3 \times 3} & 0_{3 \times 2} \\ 0_{2 \times 3} & 0_{2 \times 3} & \begin{bmatrix} 1 & T \\ 0 & 1 \end{bmatrix} \end{bmatrix} \quad H = \begin{bmatrix} \hat{a}_1 & 0_{1 \times 3} & -1 & 0 \\ \vdots & \vdots & \vdots & \vdots \\ \hat{a}_N & 0_{1 \times 3} & -1 & 0 \\ 0_{1 \times 3} & \hat{a}_1 & 0 & -1 \\ \vdots & \vdots & \vdots & \vdots \\ 0_{1 \times 3} & \hat{a}_N & 0 & -1 \end{bmatrix} \quad (25)$$

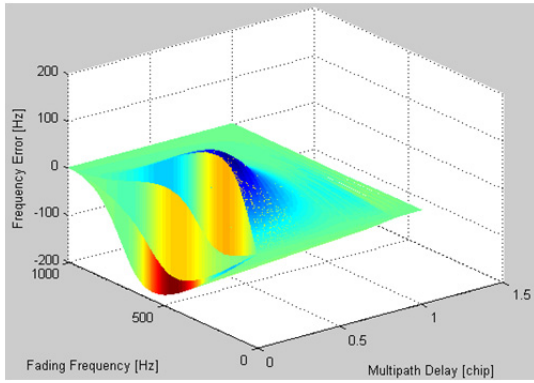
T is the update interval, $\hat{a}_i = (s_i - \hat{r}) / \|s_i - \hat{r}\|$ is a unit vector pointing from the receiver estimated position to the i^{th} satellite; $\|s_i - \hat{r}\|$ is the estimated distance between the receiver and the i^{th} satellite; $s_i = (x_i, y_i, z_i)$ is the earth-centred earth-fixed (ECEF) coordinates of the i^{th} satellite; $\hat{r} = (\hat{x}_r, \hat{y}_r, \hat{z}_r)$ is the receiver's estimated ECEF coordinates; W_k is a vector of random noise inputs such that $E\{W_k\} = 0$, $E\{W_k W_j^T\} = Q_k \delta_{kj}$; V_k is a vector of additive measurement noise such that $E\{V_k\} = 0$, $E\{V_k V_j^T\} = R_k \delta_{kj}$, $E\{W_k V_j^T\} = 0$. The EKF algorithm is as follows:

$$\left. \begin{aligned}
\hat{X}_{k|k-1} &= \Phi \hat{X}_{k-1} \\
P_{k|k-1} &= \Phi P_{k-1} \Phi^T + Q_k \\
Y_{k|k-1} &= H_k \hat{X}_{k|k-1} \\
C_k &= H_k P_{k|k-1} H_k^T + R_k
\end{aligned} \right\} \text{Prediction}$$

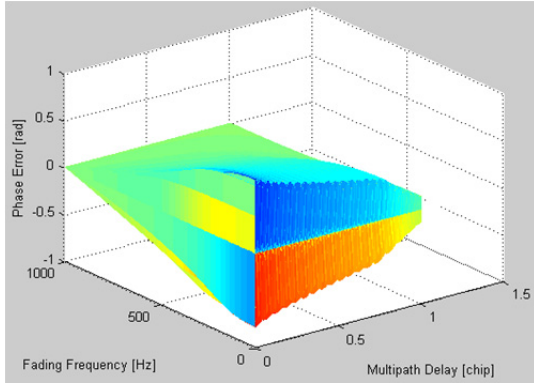
$$\left. \begin{aligned}
K_k &= P_{k|k-1} H_k^T C_k^{-1} \\
\hat{X}_k &= \hat{X}_{k|k-1} + K_k (Y_k - Y_{k|k-1}) \\
P_k &= (I - K_k H_k) P_{k|k-1}
\end{aligned} \right\} \text{Correction}$$
(26)

After the EKF has converged, the estimated state vector is [11]:

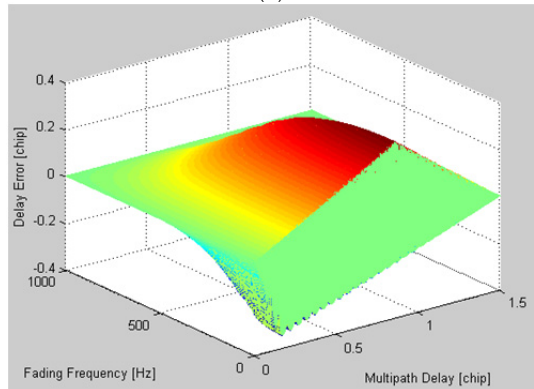
$$\hat{X}_k = P_k H_k^T R_k^{-1} Y_k \quad (27)$$



(a)



(b)



(c)

Fig. 1. Frequency (a), Phase (b) and Delay (c) Tracking Errors vs. Multipath Delay and Fading Frequency

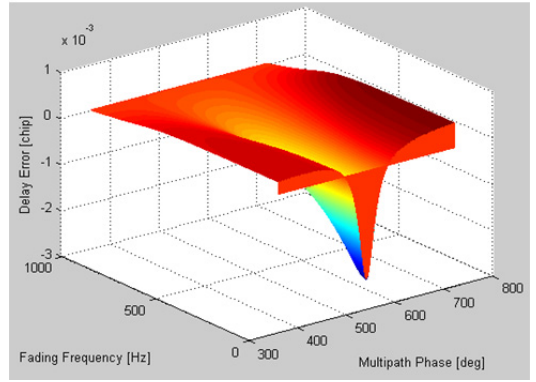
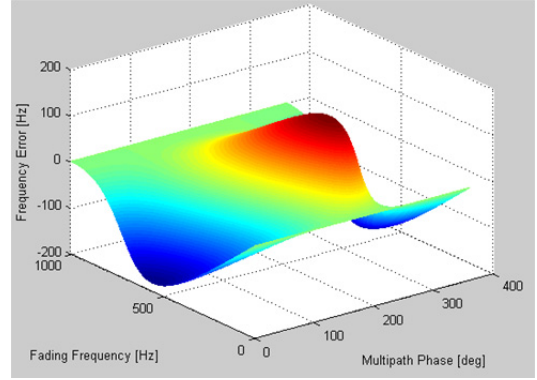
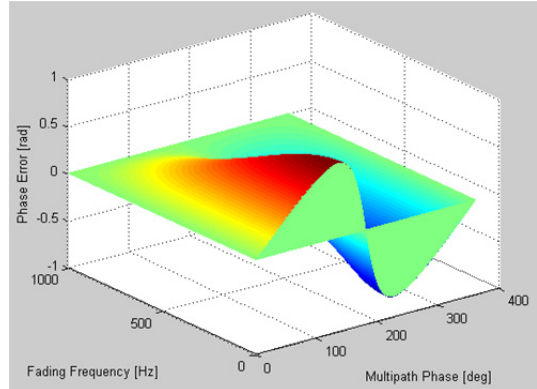


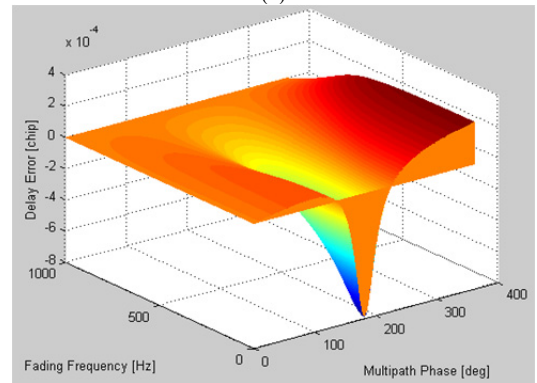
Fig. 2. Delay Tracking Error vs. Multipath Phase and Fading Frequency



(a)



(b)



(c)

Fig. 3. Frequency (a), Phase (b) and Delay (c) Tracking Errors vs. Multipath Phase and Fading Frequency

When the VDFLL is in lock, $Y_k \approx 0$ and $\hat{X}_k \approx 0$. Assuming that only the first channel is contaminated by multipath, although $Y_k \approx 0$, the real measurement vector in the presence of multipath should be $Y'_k \approx (\Delta\rho, 0, 0, \dots, \Delta\dot{\rho}, 0, 0, \dots)^T$, where:

$\Delta\dot{\rho} = -\frac{c}{f_L}\Delta f_D$ and $\Delta\rho = -\frac{c}{R_C}\Delta\tau$ as defined in Eq. (17) and Eq. (22). The corresponding real state vector is $X'_k = P_k H_k^T R_k^{-1} Y'_k$.

Assume that the SDFLL changes to VDFLL during the transition from time $k-1$ to time k , with an initial VDFLL EKF's state vector \hat{X}_{k-1} . In the absence of multipath, the state vector at time k is:

$$\begin{aligned}\hat{X}_k &= \Phi\hat{X}_{k-1} + K_k(-H_k\Phi\hat{X}_{k-1}) \\ \hat{X}_k &= (I - K_k H_k)\Phi\hat{X}_{k-1}\end{aligned}\quad (28)$$

In the presence of multipath, the state vector at time k is:

$$\begin{aligned}X'_k &= \Phi\hat{X}_{k-1} + K_k(Y'_k - H_k\Phi\hat{X}_{k-1}) \\ X'_k &= (I - K_k H_k)\Phi\hat{X}_{k-1} + K_k Y'_k\end{aligned}\quad (29)$$

The difference between the two state vectors in Eq. (28) and Eq. (29) is:

$$\Delta X_k = X'_k - \hat{X}_k = K_k Y'_k \quad (30)$$

The predicted state vector at time $k+1$ in the absence of multipath is:

$$\hat{X}_{k+1|k} = \Phi\hat{X}_k \quad (31)$$

In the presence of multipath, it is:

$$X'_{k+1|k} = \Phi(\hat{X}_k + \Delta X_k) \quad (32)$$

Thus, the error induced by multipath in the predicted state vector at time $k+1$ is:

$$\Delta X_{k+1|k} = \Phi\Delta X_k = \Phi K_k Y'_k \quad (33)$$

Similarly, the error induced by multipath in the estimated state vector at time $k+1$ is:

$$\begin{aligned}\Delta X_{k+1} &= (I - K_{k+1} H_{k+1})\Delta X_{k+1|k} + K_{k+1} Y'_{k+1} \\ \Delta X_{k+1} &= (I - K_{k+1} H_{k+1})\Phi K_k Y'_k + K_{k+1} Y'_{k+1}\end{aligned}\quad (34)$$

After the SDFLL changes to VDFLL, the code and frequency tracking errors become smaller and smaller and progressively approach their steady-state values. The initial measurement error at the time of the switch from SDFLL to VDFLL is the maximum error. Let $Y'_k \approx (\Delta\rho, 0, 0, \dots, \Delta\dot{\rho}, 0, 0, \dots)^T$ be the initial measurement vector with the maximum measurement errors. The errors induced by

multipath in the predicted and estimated state vectors at time k can be written as:

$$\begin{aligned}\Delta X_{k|k-1} &= M_{k|k-1} Y'_k \\ \Delta X_k &= M_k Y'_k\end{aligned}\quad (35)$$

$$M_{k|k-1} = \Phi M_k \quad \text{with} \quad M_k = (I - K_k H_k)M_{k|k-1} + K_k \quad (36)$$

The steady-state matrix M_{ss} is found by iteration of Equation (36) until M_k converges to a steady-state value. It is given by:

$$\begin{aligned}M_{ss} &= (I - K_{ss} H)\Phi M_{ss} + K_{ss} \\ \therefore [I - (I - K_{ss} H)\Phi]M_{ss} &= K_{ss} \\ \therefore M_{ss} &= [I - (I - K_{ss} H)\Phi]^{-1} K_{ss}\end{aligned}\quad (37)$$

where K_{ss} is the steady-state Kalman gain matrix.

The steady-state measurement vector is [11]:

$$Y'_{ss} = H\Delta X_{ss} = H M_{ss} Y'_k \quad (38)$$

Equation (38) shows that the measurement errors in Y'_k are assigned to each channel following the geometry between the satellites and the receiver to generate the new measurement errors in vector Y'_{ss} .

The steady-state multipath induced error in code delay predictions is:

$$\Delta\tau = -\frac{R_c}{c} Y'_{ss}(i), i = 1, 2, \dots, N \quad (39)$$

The steady-state multipath induced error in carrier Doppler frequency predictions is:

$$\Delta f_D = -\frac{f_L}{c} Y'_{ss}(j), j = N+1, N+2, \dots, 2N \quad (40)$$

In STL (SDFLL) tracking mode, each channel tracks a satellite independently and is unrelated to other channels. A healthy channel is therefore not affected by and does not assist a multipath-contaminated channel. In VTL (VDFLL) tracking mode however, all tracking channels are dependent on one another. When one satellite's signal is affected by a multipath signal, the other healthy channels assist the contaminated channel, and a tracking error in all channels will be induced by that single channel's multipath contamination. If another channel gets also affected by multipath, the code delay and carrier frequency errors assigned by the satellite geometry relationship among channels are directly superimposed on the errors caused by the first channel. It was demonstrated in [11] that the total multipath induced VDFLL tracking error is less than that of SDFLL, especially when more than four satellites are visible. The VTL therefore retains an advantage over the STL. There is even a more attractive way to improve VTL performance: to be able to detect a multipath contaminated channel at correlation stage and exclude it from PVT calculation. The next section discusses this notion.

IV. CORRELATOR OUTPUTS AND MULTIPATH DETECTION TECHNIQUES PLUS SIMULATION RESULTS

A. Correlator Outputs in the Presence of Multipath

A careful analysis of GPS correlator outputs in the absence and in the presence of multipath can lead to the design of multipath detection techniques. In the absence of multipath, the in-phase prompt correlator output carries the LOS signal power. In the presence of a multipath (MP) signal, the prompt correlator output is composed of the sum of the LOS and MP signals and the STL locking point is adjusted to this sum. As the tracking loop constantly seeks to bring the quadrature prompt power to zero, the quadrature prompt output will have part of the LOS + MP signal power only for a short transient time following MP arrival then will get back to zero, unless the MP signal is in phase or opposition of phase with the LOS signal. The situation in the presence of multipath is different however for early and late correlator outputs and consequently for in-phase and quadrature outputs of the coherent early-minus-late (EmL) discriminator (I_{EmL} and Q_{EmL}) as can be observed in Fig. 4 for the STL and in Fig. 5 for the VTL. The coherent EmL discriminator's equation is obtained by subtracting Eq. (5) from Eq. (4). For the STL, in the presence of multipath, the signal energy in the Q_{EmL} output during transient and steady-state times following multipath arrival is significantly higher than in the absence of multipath, unless the MP signal is in phase or opposition of phase with the LOS signal. In the absence of multipath, only noise is observed on the Q_{EmL} output.

Figures 4 and 5 represents the I_{EmL} and Q_{EmL} outputs with a reduced number of oscillations in order to show their oscillatory nature within the envelopes. Instead of 1575 cycles per C/A code chip for GPS L1, 25 cycles per C/A code chip are considered. Figure 4 shows that the Q_{EmL} output is zero for some multipath phase values even in the presence of multipath. More specifically, the Q_{EmL} output is zero when the multipath signal is in phase ($\theta_M = 0^\circ + k360^\circ$) or opposition of phase ($\theta_M = 180^\circ + k360^\circ$) with the LOS signal, with k being an integer. Except for those phase values, the Q_{EmL} output in the presence of multipath oscillates along the different multipath delay values between a maximum and a minimum which depend on the multipath to LOS amplitude ratio α and on the Early-Late correlator chip spacing δ . These multipath phase values ($\theta_M = 0^\circ + k360^\circ$ and $\theta_M = 180^\circ + k360^\circ$) correspond to multipath delay values $\delta_M = nR_c / f_{L1}$ and $\delta_M = (n+0.5)R_c / f_{L1}$, with n an integer, if multipath phase is related to multipath delay using $\theta_M = 2\pi f_{L1} \delta_M / R_c$, i.e. if it is assumed that the multipath phase is only due to the differential path delay. In general, at the moment of reflection or diffraction, the multipath signal undergoes a relative phase θ_M that can be modelled using the differential path delay and reflector and antenna parameters [14] or else assumed random [15]. For the VTL, both the I_{EmL} and Q_{EmL} outputs increase in signal power in the presence of multipath as shown in Fig. 5

and when Q_{EmL} is at zero, I_{EmL} is not and vice versa. This means that for all multipath phase or delay values, the absolute value $|EmL| = \sqrt{I_{EmL}^2 + Q_{EmL}^2}$ increases in amplitude in the presence of multipath.

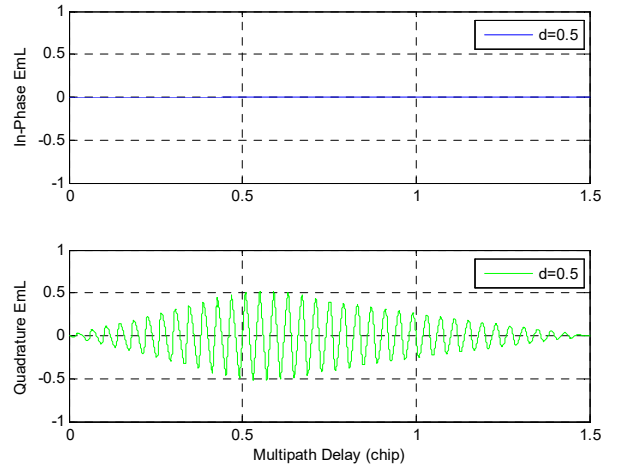


Fig. 4. I_{EmL} and Q_{EmL} amplitudes vs. Multipath delay for STL in lock (reduced oscillations, standard correlator i.e. $d=0.5$).

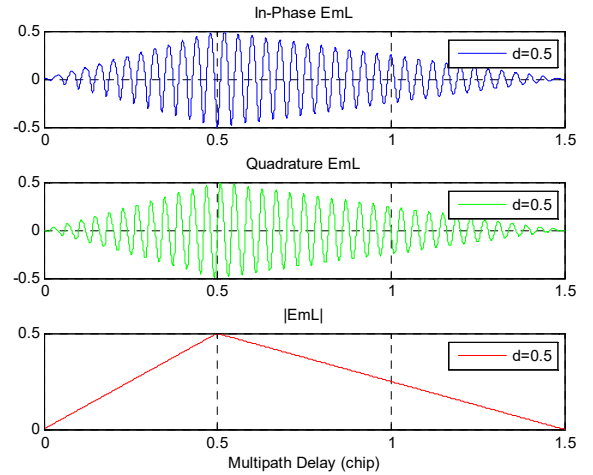
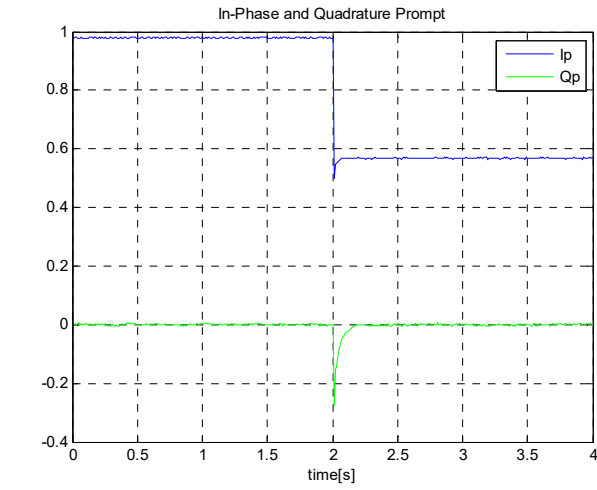
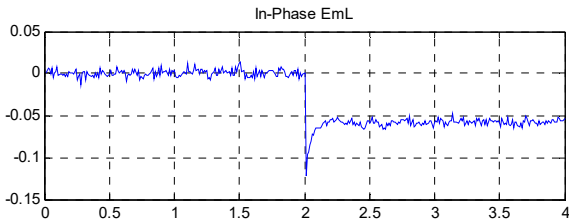


Fig. 5. I_{EmL} , Q_{EmL} and $|EmL|$ amplitudes vs. Multipath delay for VTL in lock (reduced oscillations, standard correlator i.e. $d=0.5$).

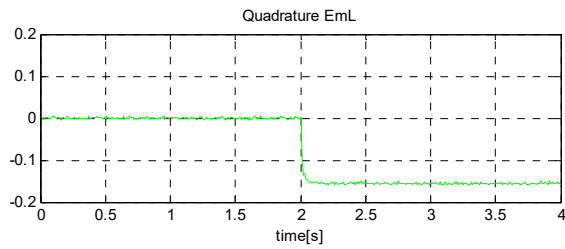
In order to further illustrate the effects of multipath on correlator outputs and analyse the possibility of devising multipath detection techniques based on them, some simulations are conducted. Consider a LOS signal to which a MP signal having the same frequency as the LOS and constant relative delay and phase values is superimposed after 2 seconds tracking time. The MP maintains these parameter values for the rest of the tracking time. The carrier to noise ratio C/N_0 is taken to be 45 dBHz. Two scenarios are studied: (1) a case where the MP increases the signal power on the Q_{EmL} arm ($\theta_M = 213^\circ$, $\delta_M = 0.1171 \text{ chip}$, $\alpha = 0.5012$) and (2) a case where it does not ($\theta_M = 0^\circ$, $\delta_M = 0.1623 \text{ chip}$, $\alpha = 0.5012$). A VTL (VDLL) tracking loop assisted by a PLL is simulated. The rest of the simulation settings are described in the labels of Figures 6 and 7.



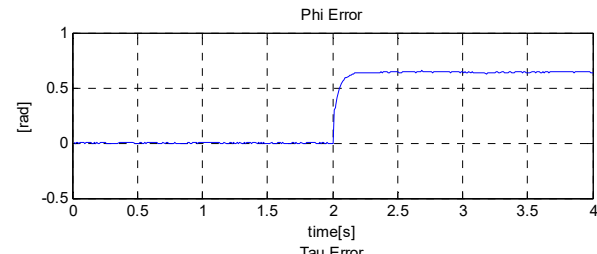
(a)



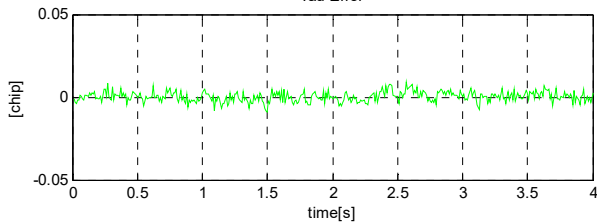
In-Phase EmL



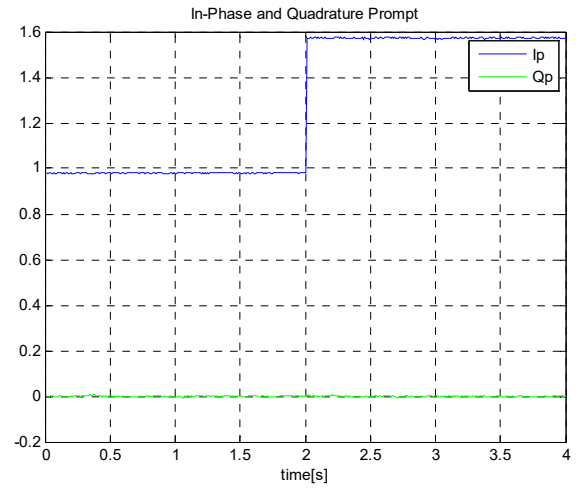
(b)



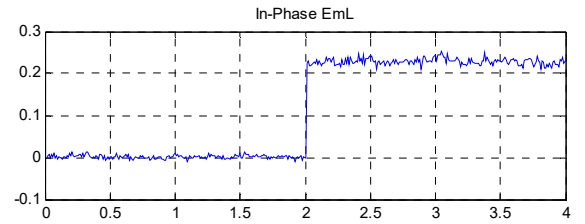
Phi Error



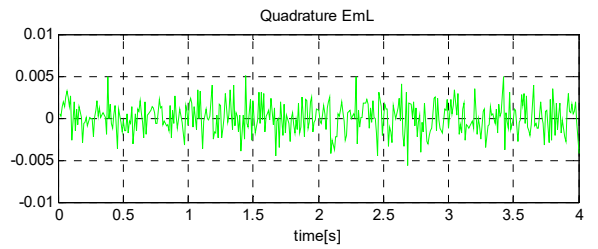
(c)



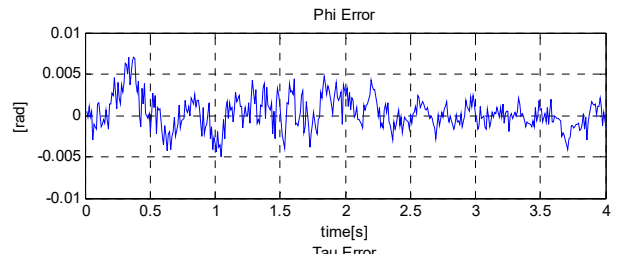
(a)



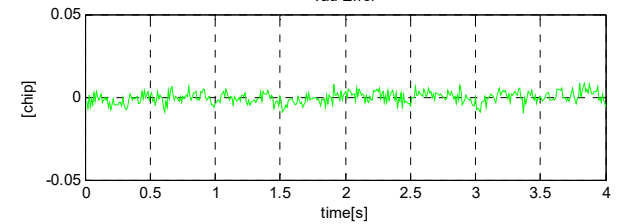
In-Phase EmL



(b)



Phi Error



(c)

Fig. 6. Tracking of LOS signal ($C/N_0=45\text{dBHz}$) and MP signal ($\theta_M = 213^\circ$, $\delta_M = 0.117\text{chip}$, $\alpha = 0.5012$) arriving after 2s tracking time for a VTL (VDLL, second order PLL, bandwidths of 1 Hz and 10 Hz respectively, coherent EmL DLL discriminator $d = 0.5\text{chip}$, ATAN PLL discriminator, coherent integration time: 10ms). A filtered autocorrelation function is used.

Fig. 7. Tracking of LOS signal ($C/N_0=45\text{dBHz}$) and MP signal ($\theta_M = 0^\circ$, $\delta_M = 0.1623\text{chip}$, $\alpha = 0.5012$) arriving after 2s tracking time for a VTL (VDLL, second order PLL, bandwidths of 1 Hz and 10 Hz respectively, coherent EmL DLL discriminator $d = 0.5\text{chip}$, ATAN PLL discriminator, coherent integration time: 10ms). A filtered autocorrelation function is used.

Figure 6 shows the results of scenario (1) for a VTL (VDLL + PLL). Figure 6(a) shows that after MP arrival, I_p arm signal power changes from a previous non-zero value to a new non-zero value and maintains its new value for the rest of the tracking period. The Q_p arm signal power on the other hand changes only for a short transient period of time before returning back to its normal value ($Q_p = 0$ for a PLL in lock). Figure 6 (b) shows that for a VTL, multipath appearance creates a change in signal power on both the I_{EmL} and Q_{EmL} arms, more on the Q_{EmL} than the I_{EmL} , for this scenario and the like. Also, the VTL whose navigator has not been seriously contaminated by multipath generally maintains the delay tracking error to a minimum value (the simulation was set to approach the behaviour $\Delta\tau \approx 0$ for a locked VDLL). This is observed in Fig. 6(c). Figure 6(c) also shows that MP induced phase error is around 0.6 rad because carrier phase is still tracked in STL mode (PLL). Therefore, I_{EmL} and/or Q_{EmL} arms can be used in multipath detection, preferably together and if useful in association with Prompt arms as well, for the VTL. In fact, these correlator outputs constitute a good mirror of MP presence for a VTL. Figure 7 depicts the results of scenario (2) for a VTL (VDLL + PLL). Figure 7(a) shows that I_p has the same behaviour as in the first scenario, but Q_p does not undergo any transient time change in value due to MP. This is due to the fact that the MP signal is in phase with the LOS signal ($\theta_M = 0^\circ$). Figure 7(b) shows that the Q_{EmL} arm for this scenario is blind to MP presence, as demonstrated in theory for this MP phase value. The I_{EmL} arm on the other hand undergoes an increase in signal power at time $t=2s$ and during the rest of the tracking period for the VTL as theorized. The STL's I_{EmL} arm in the same scenario would have a transient change in signal power before returning back to normal. Figure 7(c) show that a MP phase $\theta_M = 0^\circ$ does not induce any additional phase tracking error. Also, the VTL maintains the delay tracking error very close to zero, which is not the case for a STL in the same scenario. This second scenario shows that, for the VTL the I_{EmL} or Q_{EmL} retain the potential for multipath detection even for $\theta_M = 0^\circ$ or $\theta_M = 180^\circ$, because when these MP phase values drive the Q_{EmL} output value to zero, they do not do so for I_{EmL} and vice versa. For the STL however, both the I_{EmL} and Q_{EmL} arms are useless in multipath detection for $\theta_M = 0^\circ$ or $\theta_M = 180^\circ$, whereas those MP phase values result in maximal delay tracking errors. It appears therefore that the VTL has another advantage over the STL with regards to the potential for MP detection based on correlator outputs.

B. Multipath Detection Technique

Let EmL denote the complex output made of I_{EmL} and Q_{EmL} .

$$EmL = I_{EmL} + jQ_{EmL} = (I_E - I_L) + j(Q_E - Q_L) \quad (41a)$$

$$|EmL| = \sqrt{(I_{EmL}^2 + Q_{EmL}^2)} \quad (41b)$$

For the VTL, the presence of multipath is visible on I_{EmL} and/or Q_{EmL} outputs as long as the navigation filter is not contaminated. A binary hypothesis test can be defined assuming that the multipath exists for a sufficient time and that its complex amplitude A does not change for an observation window of N samples and of initial index n_0 .

$$H_0: EmL(n) = w_{EmL}$$

$$H_1: EmL(n) = A + w_{EmL}, \text{ with } n \in \{1, \dots, N\} + n_0$$

Assuming that A and σ^2 (the variance of w_{EmL}) are unknown, a generalized likelihood ratio test (GLRT) [16] to decide for H_0 or H_1 can be formulated as:

$$\frac{\overline{EmL}^2}{\hat{\sigma}^2} > \eta \quad \text{or} \quad \frac{\overline{EmL}^2}{\hat{\sigma}^2} < \eta \quad (42)$$

where η is the detection threshold, \overline{EmL} is the mean of the N samples on the EmL correlation point of the VTL and $\hat{\sigma}^2$ is the ML estimator of the noise power under hypothesis H_1 .

$$\overline{EmL} = \frac{1}{N} \sum_{n=1}^N EmL(n + n_0) \quad (43a)$$

$$\hat{\sigma}^2 = \frac{1}{N} \sum_{n=1}^N |EmL(n + n_0) - \overline{EmL}|^2 \quad (43b)$$

The detection threshold is

$$\eta = \exp\left\{\frac{[cdf^{-1}(1 - PFA/2)]^2}{N}\right\} - 1 \quad (44)$$

with cdf being the cumulative distribution function of the standard normal distribution, cdf^{-1} the inverse cumulative distribution function, and PFA the probability of false alarm. The values of PFA and N have a great impact on the performance of the detector, and there is a trade-off between obtaining a high detection capability or a low false alarm rate. Increasing the value of N and/or PFA improves the detection capability of the GLRT in theory. However, in practice, increasing the value of N delays the instant when the multipath is detected and may go against the assumption that the amplitude A of the multipath remains constant for the duration of N samples. On the other hand, increasing PFA may result in many false detections and this may not be beneficial if the objective is to exclude the multipath contaminated satellites from the navigation solution. One might wind up with fewer satellites than needed to compute the PVT solution. If N is assumed sufficiently large ($N > 30$), the probability of detection (PD) is given by

$$\begin{aligned}
PD = & 2 - cdf\left(cdf^{-1}\left(1 - \frac{PFA}{2}\right) - \sqrt{SNR}\right) \\
& - cdf\left(cdf^{-1}\left(1 - \frac{PFA}{2}\right) + \sqrt{SNR}\right)
\end{aligned} \quad (45)$$

where SNR is the post-correlation signal to noise ratio and is given by $SNR = \frac{N|A|^2}{\sigma^2}$. This PD depends on the chosen PFA, on the modulus of the amplitude A of the EmL output, and on the noise power on that output. This noise power is given by $\sigma^2 = \sigma_n^2 K(1-r)$ [17] where $\sigma_n^2 = N_0 f_s$ is the thermal noise power (N_0 and f_s are noise spectral density and baseband sampling frequency respectively), K is the number of correlation points, and $r = 1 - 2d$ is the level of correlation between the Early and Late outputs. From $A_0 = \sqrt{C} K \sin c(\pi \Delta f T)$ with $A_M = \alpha A_0$, the post-correlation SNR at the EmL output has thus the following expression linking it to the carrier-to-noise ratio (C/N_0):

$$\begin{aligned}
SNR = & \frac{NA^2}{2\sigma^2} = \frac{C}{N_0} \frac{NT}{2} \frac{\sin^2(\pi \Delta f T)}{2d} \times \\
& \left[\left\{ \begin{aligned} & [R(\Delta\tau + d) - R(\Delta\tau - d)] \cos(\Delta\varphi) + \\ & \alpha [R(\Delta\tau - \delta_M + d) - R(\Delta\tau - \delta_M - d)] \cos(\Delta\varphi - \theta_M) \end{aligned} \right\}^2 + \right. \\
& \left. \left\{ \begin{aligned} & [R(\Delta\tau + d) - R(\Delta\tau - d)] \sin(\Delta\varphi) + \\ & \alpha [R(\Delta\tau - \delta_M + d) - R(\Delta\tau - \delta_M - d)] \sin(\Delta\varphi - \theta_M) \end{aligned} \right\}^2 \right]
\end{aligned} \quad (46)$$

where C is the LOS power before correlation, T the coherent integration time ($K = Tf_s$) and Δf the error between the LOS carrier frequency and the estimated carrier replica frequency.

Figures 8 to 11 illustrates the results of simulations used to validate the proposed detection technique. The two ray multipath model (LOS + 1 MP) is used in the simulations. A multipath signal is set to appear after 2 seconds tracking time for one channel of a VTL (VDLL + second order PLL, bandwidths of 1 Hz and 10 Hz respectively, coherent EmL DLL discriminator $d = 0.5 \text{ chip}$, ATAN PLL discriminator, coherent integration time: 10ms). The C/N_0 is set to 45 dBHz, a value corresponding to good satellite signal reception. A PFA of 10^{-4} is used to set the detection threshold using Eq. (44). A sliding window of $N = 30$ samples (corresponding to 30 ms time delay before the first detection for a coherent integration time of 10 ms) is used to set the detection test. The suggested GLRT detector metric (see Eq. 42) goes beyond threshold once a multipath signal appears and is superimposed onto the LOS signal (shortly after 2s tracking time) proving that the detection technique performs well. This holds true even for multipath arriving in phase ($\theta_M = 0^\circ$) or opposition of phase ($\theta_M = 180^\circ$) with the LOS signal as shown in Fig. 9 and Fig. 11 because though the Q_{EmL} output is blind to such MP, the I_{EmL} output is not for a VTL with a non-contaminated navigation filter contrarily to a STL.

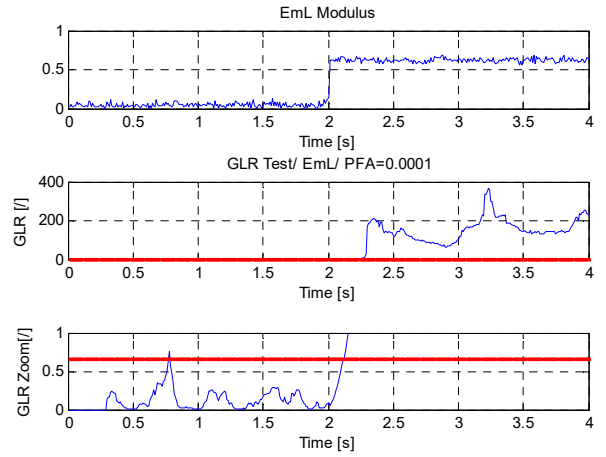


Fig. 8. Detection of MP signal ($\theta_M = 94.32^\circ$, $\delta_M = 0.6203 \text{ chip}$, $\alpha = 0.5012$) arriving after 2s tracking time for a VTL (VDLL + PLL), $C/N_0 = 45 \text{ dBHz}$.

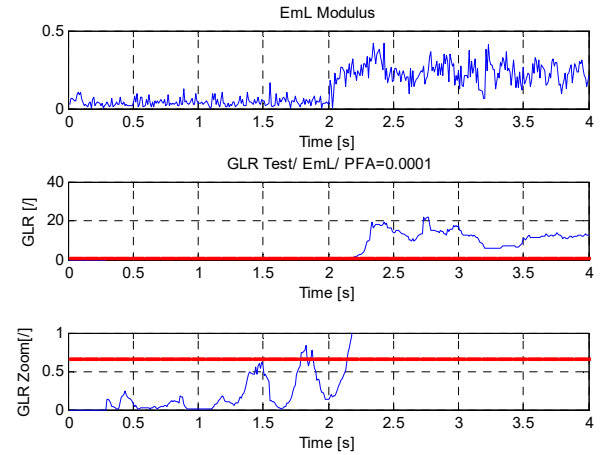


Fig. 9. Detection of MP signal ($\theta_M = 0^\circ$, $\delta_M = 0.1623 \text{ chip}$, $\alpha = 0.5012$) arriving after 2s of tracking for a VTL (VDLL + PLL), $C/N_0 = 45 \text{ dBHz}$.

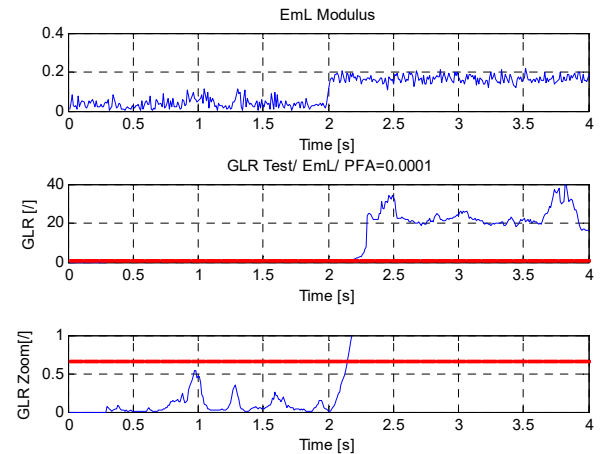


Fig. 10. Detection of MP signal ($\theta_M = 213^\circ$, $\delta_M = 0.1171 \text{ chip}$, $\alpha = 0.5012$) arriving after 2s tracking time for a VTL (VDLL + PLL), $C/N_0 = 45 \text{ dBHz}$.

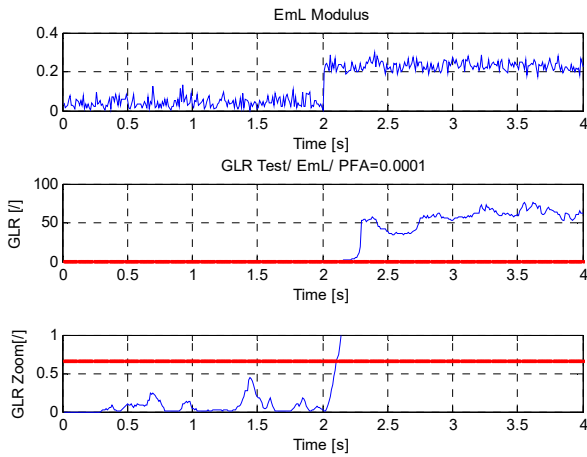


Fig. 11. Detection of MP signal ($\theta_M = 180^\circ$, $\delta_M = 0.1623\text{chip}$, $\alpha = 0.5012$) arriving after 2s tracking time for a VTL (VDLL, second order PLL, bandwidths of 1 Hz and 10 Hz respectively, coherent EmL DLL discriminator $d = 0.5\text{chip}$, ATAN PLL discriminator, coherent integration time: 10ms, $C/N_0 = 45\text{dBHz}$).

V. CONCLUSION

This paper provides characterisation of multipath induced tracking errors for the VTL. The paper contributes to the characterization of tracking and positioning errors for VTLs by deriving models that allow the analysis of both code and carrier tracking errors with respect to multipath delay, multipath phase and multipath fading frequency. The VTL (VDFLL) initial tracking error models correspond exactly to the STL (SDFLL) error models. The error values for the VDFLL however go decreasing as the VDFLL's EKF converges and they reach their steady-state values. Moreover, the paper provides an analysis for devising multipath detection techniques based on correlator outputs. This analysis is performed using simulations of the VTL. It is proved that the I_{EmL} and/or Q_{EmL} correlator outputs constitute a good mirror of MP presence for the VTL and therefore can be used to formulate MP detection techniques. The Q_{EmL} correlator output can be used to define MP detection techniques for the STL as well except when the MP signal is in phase ($\theta_M = 0^\circ + k360^\circ$) or opposition of phase ($\theta_M = 180^\circ + k360^\circ$) with the LOS signal. The VTL therefore retains another advantage over the STL. The paper then provides a simple multipath detection technique based on the previous analysis and using a generalized maximum likelihood ratio test (GLRT), and illustrates its validity through simulations.

REFERENCES

- [1] D.-J. Moelker, "Multiple antennas for advanced gnss multipath mitigation and multipath direction finding," *Proceedings of ION GPS-97*, September 1997.
- [2] G. Brodin, "GNSS Code and Carrier Tracking in the Presence of Multipath," *Proc. ION GPS-96*, pp. 1389-1398, 1996.
- [3] L. Liu and M. Amin, "Comparison of Average Performance of GPS Discriminators in Multipath," *Proc. IEEE ICASSP 2007*, pp. 1285-1288, 2007.
- [4] J. Chen, L. Cheng and M. Gan, "Modeling of GPS Code and Carrier Tracking Error in Multipath," *Chinese Journal of Electronics*, vol. 21, no. 1, pp. 78-84, January 2012.
- [5] J. Chen, L. Cheng and M. Gan, "Model and Simulation of Multipath Error in DLL for GPS Receiver," *Chinese Journal of Electronics*, vol. 23, no. 3, pp. 508-515, July 2014.
- [6] Y. Wang, R. Yang, K. V. Ling and E. K. Poh, "Robust Vector Tracking Loop Using Moving Horizon Estimation," in *Proceedings of the ION 2015 Pacific PNT Meeting*, Honolulu, Hawaii, April 2015.
- [7] S. Bhattacharyya and D. Gebre-Egziabher, "Development and validation of a parametric model for vector tracking loops," in *22nd International Technical Meeting of the Satellite Division of the Institute of Navigation 2009, ION GNSS 2009*, Savannah, GA, 2009.
- [8] N. Kanwal, "Vector tracking loop design for degraded signal environment (Master Thesis)," Tampere University of Technology, Tampere, Finland, 2010.
- [9] M. Lashley and D. Bevly, "Comparison of Traditional Tracking Loops and Vector Based Tracking Loops for Weak GPS Signals," in *ION GNSS 20th International Technical Meeting of the Satellite Division*, Fort Worth, TX, 2007.
- [10] S. Peng, Y. Morton and R. Di, "A multiple-frequency GPS software receiver design based on a vector tracking loop," in *2012 IEEE/ION Position, Location and Navigation Symposium (PLANS)*, 2012.
- [11] Y. Luo, Y. Wang, S. Wu and P. Wang, "Multipath effects on vector tracking algorithm for GNSS signal," *Science China, Information Sciences*, vol. 57, October 2014.
- [12] M. Lashley and D. Bevly, "Analysis of discriminator based vector tracking algorithms," in *Proceedings of the National Technical Meeting of The Institute of Navigation*, San Diego, 2007.
- [13] J.-M. Sleewaegen, "Multipath Mitigation, Benefits from using the Signal-to-Noise Ratio," in *Proceedings of the 10th International Technical Meeting of the Satellite Division of The Institute of Navigation (ION GPS 1997)*, Kansas City, MO, September 16-19, 1997.
- [14] J. Ray, "Mitigation of GPS Code and Carrier Phase Multipath Effects Using a Multi-Antenna System," *PhD Thesis*, March 2000.
- [15] V. Heiries, "Optimisation d'une chaîne de réception pour signaux de radionavigation par satellite à porteuse à double décalage (BOC)," *PhD Thesis*, 2007.
- [16] Kay, S., *Fundamentals of statistical signal processing, Volume II: Detection theory*, Prentice Hall, 1998.
- [17] A. Dierendonck, P. Fenton and T. Ford, "Theory and Performance of Narrow Correlator Spacing in a GPS Receiver," *NAVIGATION, Journal of the Institute of Navigation*, vol. 39, no. 3, pp. 265-283, 1992.